Article

Surface-Enhanced Raman Spectroscopy for Monitoring the Biochemical Changes Due to DNA Mutations Induced by CRISPR-Cas9 Genome Editing in the *Aspergillus niger* Fungus

Muhammad Wasim,[∥] Usman Ghaffar,[∥] Muhammad Rizwan Javed,* Haq Nawaz,*
Muhammad Irfan Majeed,* Anam Ijaz, Shazra Ishtiaq, Nimra Rehman, Rabeea Razaq, Sobia Younas,
Aqsa Bano, Naeema Kanwal, and Muhammad Imran

Cite This: *ACS Omega* 2024, 9, 15202−15209

Read Online

ACCESS | Metrics & More | Article Recommendations

ABSTRACT: In this study, surface-enhanced Raman spectroscopy (SERS) technique, along with principal component analysis (PCA) and partial least-squares discriminant analysis (PLS-DA), is used as a simple, quick, and cost-effective analysis method for identifying biochemical changes occurring due to induced mutations in the *Aspergillus niger* fungus strain. The goal of this study is to identify the biochemical changes in the mutated fungal cells (cell mass) as compared to the control/nonmutated cells. Furthermore, multivariate data analysis tools, including PCA and PLS-DA, are used to further confirm the differentiating SERS spectral features among fungal samples. The mutations are caused in *A. niger* by the clustered regularly interspaced palindromic repeat CRISPR-Cas9 genomic editing method to improve their biotechnological potential for the production of cellulase enzyme. SERS was employed to detect the changes in the cells of mutated *A. niger* fungal strains, including one mutant producing low levels of an enzyme and another mutant producing high levels of the enzyme as a result of mutation as compared with an unmutated fungal strain as a control sample. The distinctive features of SERS corresponding to nucleic acids and proteins appear at 546, 622, 655, 738, 802, 835, 959, 1025, 1157, 1245, 1331, 1398, and 1469 cm^{-1}. Furthermore, PLS-DA is used to confirm the 89% accuracy, 87.7% precision, 87% sensitivity, and 88.9% specificity of this method, and the value of the area under the curve (AUROC) is 0.67. It has been shown that surface-enhanced Raman spectroscopy is an effective method for identifying and differentiating biochemical changes in genome-modified fungal samples.

1. INTRODUCTION

A fungus is one of the most diverse families of heterotrophic organisms on this planet. There are an estimated 1.5 million species, of which 70,000 have been described.[1] *Aspergillus niger* is a thermotolerant, saprophytic,[2] and incredibly common filamentous ascomycete fungus associated with human parasitic infections.[3] Numerous fungi have been used for various purposes, including in industrial and medicinal applications, biotechnology, experimental model systems, and maintaining ecosystem stability. The recycling of organic plant components by fungi is vital for the environment and is important in the production of food, pharmaceuticals, and industry. Fungi are also essential living organisms that can break down lignin and cellulose, which is vital for the ecosystem.[4] Some species may have negative impacts on humans by spreading dangerous diseases or spoiling food.

Filamentous fungi play a significant role in biotechnology as sources of enzymes and various other natural compounds used in the production of medicines, pigments, and biofuel. The extraction or production of cellulase enzyme using *A. niger* is the most economical route. As *A. niger* is ubiquitous in the atmosphere, it is easy to operate for cellulase production.[5] As cellulase eliminates the antinutritional components of the feed, they are utilized in feed manufacturing for animals.[6] The cost of cellulase enzyme is increasing continuously, and its efficient production at a higher scale is required.[7] Therefore, it is necessary to improve the activity and production of the cellulase enzyme. For this purpose, mutation can be caused in a desired species such as *A. niger,* as this fungus has long been the target of genetic selection and genome editing to improve its biotechnological potential.
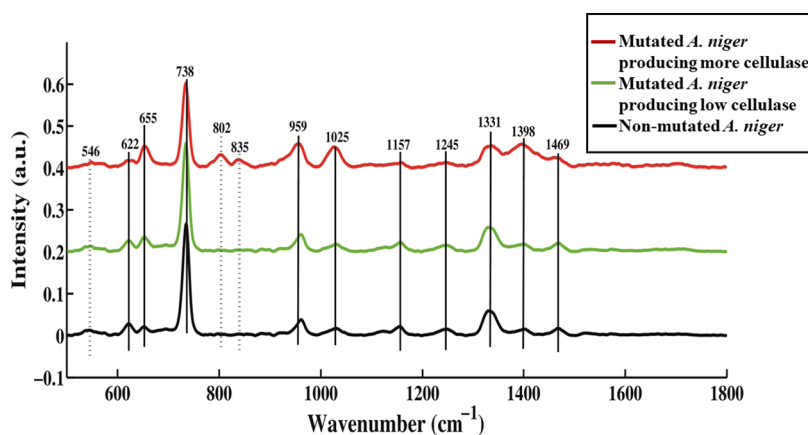
Figure 1. Comparison of the mean SERS spectra of unmutated *A. niger* with the two mutated variants, one exhibiting less cellulase enzyme production and the other with increased cellulase production.

The CRISPR-Cas9 genome editing method has been recognized in *A. niger* species due to its significance in biotechnology, food and nutrition security, and human health impact.[8] In order to initiate Cas9-mediated genome editing, the nucleus of the target organism must comprise both the endonuclease and the single guide RNA (sgRNA). Transformation strategies have been successfully used for the introduction of Cas9 and sgRNA in filamentous fungi. There are three main methods of delivering Cas9 and sgRNA, including alteration of the DNA encoding Cas9, alteration of in vitro-transcribed sgRNAs, and modification of a preassembled CRISPR-Cas9/sgRNA ribonucleoprotein (RNPs) complex. After conversion, the Cas9 gene can either be directed to specific sites in the genome or integrated at random positions.[8] Given its versatile nature, understanding the genetic makeup of *A. niger* has become crucial for enhancing its utility in biotechnological processes.

The characterization of the fungal morphology and cell structures has been performed using microscopy techniques (fluorescence microscopy, confocal laser scanning microscopy, atomic force microscopy, and ultraviolet (UV), light, and electron microscopy).[2] These techniques are employed to gain insights related to the physiology and structure of fungi.[9] However, the results obtained by the optical microscopy technique are not clear enough to classify the various species of *Aspergillus* having minute differences. In addition to microscopy, various spectroscopic techniques, including ultraviolet—visible (UV—vis) spectroscopy,[10] one-dimensional nuclear magnetic resonance (1D-NMR) spectroscopy,[11] and infrared (IR) spectroscopy,[12] are more widely used to speed up the analysis process. NMR technique can indeed provide valuable information about cellular transformations, but it is labor-intensive, expensive, and requires careful preparation of samples. Infrared (IR) spectroscopy has some limitations, such as in the case of biological samples, it strongly absorbs water, which can lead to significant interference.[13] To address these constraints, it is essential to develop efficient, affordable, and noninvasive methods.

Raman spectroscopy is a quick and low-cost analytical method that does not require extensive sample preparation. It offers molecular fingerprints, which can be used to determine the structure and molecular composition of the fungi.[4,14,15] This technique is accurate, reliable, and rapid for the identification and discrimination of various species, but it cannot be used in microbiological detection due to the weak

signal, fluorescent background, and low sensitivity.[16] To overcome these limitations, surface-enhanced Raman spectroscopy (SERS) is performed, which amplifies the Raman signal through SERS-active substrates, such as roughened coinage metal surfaces, enabling fungal identification and detection.[15,17,18] SERS provides single-molecule structural details by strong electromagnetic field amplification through localized surface plasmon (LSP) excitation. Some obvious advantages of SERS compared with traditional Raman spectroscopy are signal enhancement by several orders, quenching of the fluorescence background, and improvement of the signal-to-noise ratio.[19]

In this study, the CRISPR-Cas9 technique was employed on *A. niger*. The SERS technique was employed for the rapid detection and identification of *A. niger* fungal DNA in a quick and effective manner by using silver nanoparticles as a SERS substrate. The SERS technique enables the detection of subtle biochemical changes between the nonmutated and two different mutated strains with varying cellulase enzyme production levels. PCA and PLS-DA are also used for rapid discrimination among SERS spectral data sets of mutated and nonmutated *A. niger* strains. A comprehensive literature review reveals that no previous studies have explored this specific area of research.

2. RESULTS AND DISCUSSION

2.1. Characterization of Ag NPs. Lab-synthesized silver nanoparticles were characterized through scanning electron microscopy (SEM)[20] and transmission electron microscopy (TEM) techniques. By controlling their refractive index, size, and shape, their scattering and absorption properties can be varied.[21] Nanoparticles (NPs) with a rough surface make a greater contribution toward SERS enhancement as compared to NPs with a smooth surface. The characterized silver nanoparticles have an oval-shaped geometry, with a size of 65 nm × 45 nm, as shown in the Supporting Information.[22,23]

2.2. Mean SERS Spectra. SERS is employed to analyze the spectral characteristics of the *A. niger* cell mass under different conditions, with SERS spectra recorded for three samples in the range of 500–1800 cm⁻¹, as presented in Figure 1. It depicts a comparison between the mean SERS spectra of control *A. niger* (black spectra), mutated *A. niger* with low cellulase enzyme production (green spectra), and mutated *A. niger* with more cellulase enzyme production (red spectra). More prominent SERS features are marked as solid and dotted

lines. Solid lines denote features that represent intensity differences, while dotted lines denote features that appear in the mutated *A. niger* but are absent in the nonmutated *A. niger*. Interpreting alterations in cellular components, specifically nucleic acids and proteins, provides insights into the biochemical changes occurring in *A. niger*.

The SERS bands reported in the literature are used for the peak assignment of the spectral features for the interpretation of results as described in Table 1 with related references.

Table 1. Peak Assignments for the SERS Spectral Data Sets of the Nonmutated and Mutated *A. niger* Samples with Low and High Cellulase Production Levels

wavenumbers (cm^{-1})	SERS peak assignment	components	refs
546	S−S stretching	protein	26
622	cytosine	nucleic acid	4
655	guanine (ring breathing)	nucleic acid	24
738	a glycosidic ring breathing	nucleic acid	24
802	uracil ring breathing mode of DNA	nucleic acid	26
835	thymine	nucleic acid	28
959	C=C deformation	protein	29
1025	C−O vibration	protein	26
1157	−C−N− aromatic amino acid	protein	24
1245	thymine	nucleic acid	28
1331	guanine deformation	nucleic acid	24
1398	CH$_2$ distortion	protein	30
1469	adenine	nucleic acid	27

Distinctive SERS bands associated with nucleic acids were observed across the spectrum. Notable bands at 622 cm^{-1} (cytosine), 655 cm^{-1} (guanine), 738 cm^{-1} (glycosidic ring breathing), 802 cm^{-1} (uracil), 835 cm^{-1} (thymine), 1245 cm^{-1} (thymine), 1331 cm^{-1} (guanine deformation), and 1469 cm^{-1} (adenine) were detected.

The SERS band exhibiting a reduced intensity at 622 cm^{-1} is linked to cytosine, the band at 1245 cm^{-1} is attributed to thymine, and the band at 1469 cm^{-1} is attributed to adenine. Conversely, the significantly increased intensity at 1331 cm^{-1} (guanine deformation) suggests a potential association with nucleic acid degradation and nucleotide release due to cellular starvation, leading to the extracellular release of adenine and guanine.[24]

The SERS peaks exhibiting significantly increased intensities in mutated *A. niger* at 655 cm^{-1} (guanine ring breathing), 738 cm^{-1} (glycosidic ring breathing), 802 cm^{-1} (uracil ring breathing), and 835 cm^{-1} (thymine) indicated the destruction of certain DNA content in the fungal mycelia after the mutation, which leads to higher enzyme production. Moreover, adenine acts as the basis for the production of adenosine triphosphate in the cells and supplies the energy needed for cellular growth. After exposure, the intensity decreased, which meant that the energy sources for cell growth were destroyed.[25]

SERS bands related to proteins exhibited noticeable changes in the mutated *A. niger* strains. Increased intensity at 546 cm^{-1} (S−S stretching), 959 cm^{-1} (C−C−N stretching), and 1025 cm^{-1} (C−O vibration) indicated alterations in the protein structure. The CH$_2$ deformation of proteins, observed at 1398 cm^{-1}, further highlighted variations in the protein composition.[26] The decrease in intensity at 1157 cm^{-1} (C−N stretching in aromatic amino acids) suggests structural changes in proteins, possibly due to oxidative stress or the degradation of protein backbones. The weakened SERS response to cell wall carbohydrates implies a stronger interaction between the cell wall and proteins, emphasizing the significance of phenylalanine in the fungal outer layers and inner walls.[27] The observed alterations in the SERS bands suggest significant biological implications.

The identified SERS bands associated with nucleic acids and proteins serve as indicators of cellular processes including DNA degradation, protein modification, and potential cellular starvation, providing a deeper understanding of the molecular dynamics within the fungal cells under varying cellulase enzyme production levels.

2.3. Principal Component Analysis (PCA). Multivariate statistical approaches are required to reveal hidden relationships between biochemical parameters and establish relevant characteristics for classification and grouping.[15] Therefore, principal component analysis (PCA) was applied to SERS spectral data in order to further explore the variability of SERS spectra to differentiate between the nonmutated and mutated *A. niger* samples. The scatter plot makes it evident that different variants of fungal cell strains are clustered in distinct locations. Although there is variability among samples, data related to a specific fungal strain remain clustered separate from other variants. The preprocessed spectral data (back-
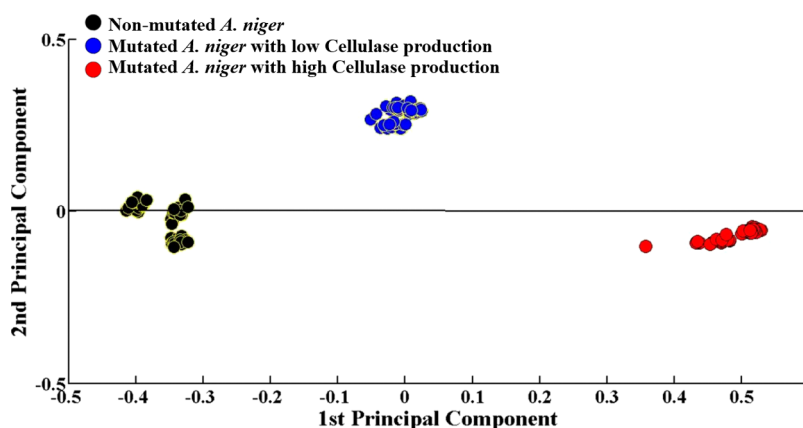

Figure 2. PCA scatter plot of SERS spectral data sets of the nonmutated and mutated *A. niger* samples with low and high cellulase production levels.
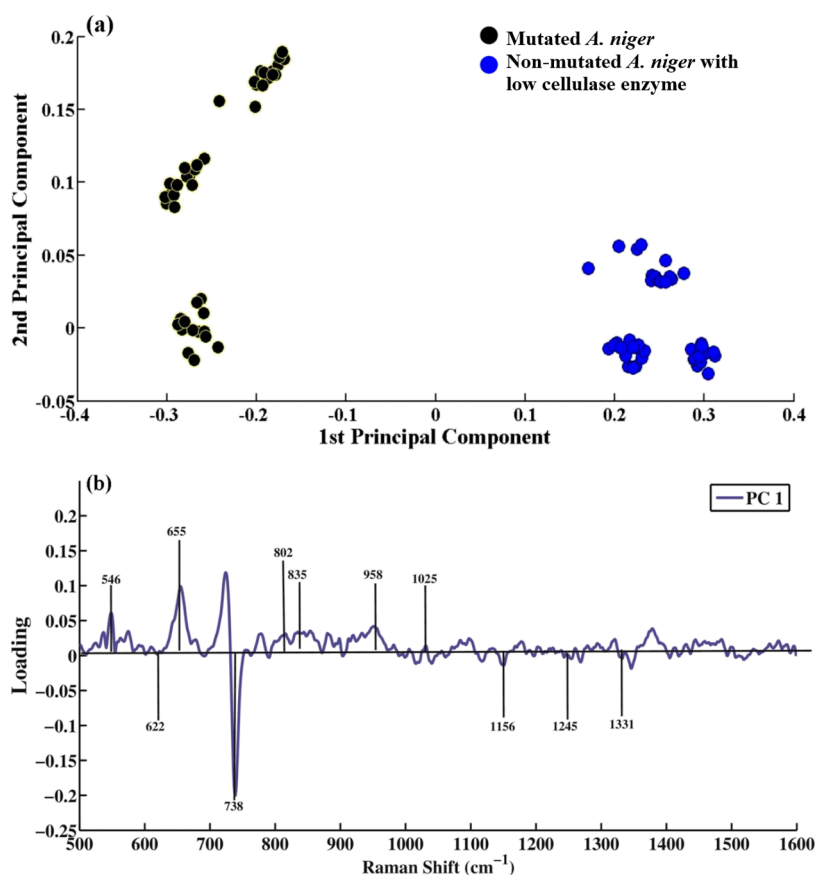
Figure 3. (a) PCA scatter plot and (b) PCA loadings of SERS spectral data sets of the nonmutated and mutated *A. niger* with low cellulase enzyme production.

grounded, smoothed, baseline-corrected, and normalized) in the whole spectral region of 400−1800 cm^{-1} were used.

Figure 2 shows the PCA scatter plot with three distinct clusters of SERS data sets of the nonmutated *A. niger* and mutated *A. niger* samples with low and high cellulase enzyme production. The spectral data of nonmutated *A. niger* samples are clustered on the negative *x*-axis, as presented by black dots, and mutated *A. niger* samples are clustered on the positive side, as indicated by red and blue dots. A clear differentiation of these mutated and nonmutated *A. niger* species is indicated by PC-1, explaining the 97.5% variance in the SERS data.

2.4. Pairwise PCA Analysis. Pairwise PCA is performed to further investigate the differentiation potential of SERS and identify the biochemical characteristics that allow for the differentiation between the spectral data sets of nonmutated and mutated fungal strains.

The PCA score plot displayed in Figure 3a compares nonmutated *A. niger* and mutated *A. niger* with low enzyme production by two distinct clusters. Blue clusters on the positive side of the *x*-axis are associated with mutated *A. niger* producing low enzyme, while black dots on the negative side of the *x*-axis can be related to unmutated *A. niger*. PC-1 explains the 99.47% variability, while PC-2 explains the 0.53% variability in the SERS spectral data sets of fungal strains. Figure 3b illustrates the PCA loadings of SERS spectral data sets of nonmutated *A. niger* and mutated *A. niger* with low enzyme production. The PCA loading refers to the coefficients of the linear combinations that constitute the principal components in PCA and are essential for understanding the contribution of each original variable to the principal

components. The SERS bands at 546 cm^{-1} (S−S stretching), 655 cm^{-1} (guanine ring breathing), 802 cm^{-1} (uracil ring breathing mode of DNA/RNA), 835 cm^{-1} (thymine), 959 cm^{-1} (C═C deformation), and 1025 cm^{-1} (C−O vibration) are associated with positive loadings of mutated *A. niger* producing low levels of the cellulase enzyme. Thus, these characteristic features are SERS biomarkers of the mutated *A. niger* (with low cellulase enzyme production level) having data clustered on the positive side of PC-1 in the scatter plot. The mean plot also indicates that the mutated *A. niger* variant (with low cellulase enzyme production levels) exhibits a higher content of these biomolecules as compared to the nonmutated fungal strain. The SERS spectral features at 622 cm^{-1} (cytosine), 738 cm^{-1} (glycosidic ring breathing), 1157 cm^{-1} (C−N str. in amino acids), 1245 cm^{-1} (thymine), and 1331 cm^{-1} (A&G, deformation) correspond to negative loading of the nonmutated fungal variant, and they correspond to the SERS spectral features of the mean plot, as displayed in Figure 1.

A comparison between the spectral data of nonmutated *A. niger* and mutated *A. niger* producing more cellulase enzyme is shown in Figure 4a. For the differentiation by using these two SERS data sets, PCA offers a 99.4% explanation of the variability as the red clusters on the positive side of the *x*-axis are related to mutated *A. niger* with more enzyme production and the black dots on the negative side of the *x*-axis are associated with nonmutated *A. niger*. Figure 4b displays the PCA loadings of SERS data sets of nonmutated *A. niger* and mutated *A. niger* with high cellulase enzyme production. PC-1 is used to determine the variability of SERS spectral features of
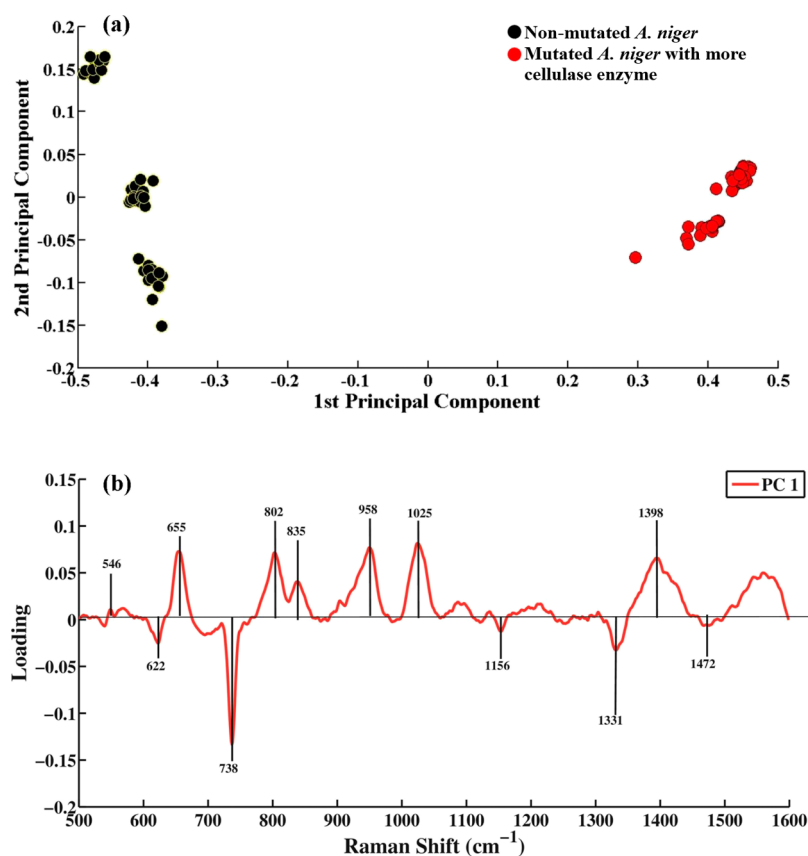
Figure 4. (a) PCA scatter plot and (b) PCA loadings of SERS spectral data sets of nonmutated *A. niger* and mutated *A. niger* with high cellulase enzyme production.

nonmutated *A. niger* and mutated *A. niger* with high enzyme production. The positive loadings comprise 546 cm^{-1}(S−S stretching), 655 cm^{-1} (guanine ring breathing), 802 cm^{-1} (uracil ring breathing), 835 cm^{-1} (thymine), 959 cm^{-1} (C═C deformation), 1025 cm^{-1} (C−O vibration), 1398 cm^{-1} (CH$_2$ stretching), and the C−N stretching of phospholipids, observed in the mean spectra of mutated strains with high enzyme production. Thus, these characteristic features are SERS biomarkers of the mutated *A. niger* (with high cellulase enzyme production levels) having data clustered on the positive side of PC-1 in the scatter plot. However, peaks observed on the negative side at 622 cm^{-1} (cytosine), 738 cm^{-1} (glycosidic ring breathing), 1157 cm^{-1} (C−N stretching), 1331 cm^{-1} (A&G deformation), and 1469 cm^{-1} (adenine) belong to the nonmutated *A. niger* sample. These results are in accordance with the mean spectra and indicate the potential of PCA as a tool for differentiation among spectral data of different mutated and nonmutated *A. niger* fungal strains.

2.5. Partial Least-Squares Discriminant Analysis (PLS-DA). PLS-DA is a multivariate statistical tool that is employed with the SERS spectral data for predictive and descriptive modeling along with the data classification into different sets to classify various levels of mutations. PLS-DA has been used for the differentiation of both types of mutated samples. Moreover, this method can distinguish variations and classify various groups. PLS-DA allows the selection of the most prominent features in the spectral data, which is useful in the classification of samples.

In order to develop the PLS-DA model, the whole data was split into 60% calibration and 40% validation data sets. In order to obtain good accuracy, the MONTE-CARLO validation was performed, and the optimal number of latent variables (OptLVs) was found to be 7. Nonmutated *A. niger* and mutated *A. niger* were discriminated by using PLS-DA with 87% sensitivity, 89% accuracy, 87.7% precision, and 88.9% specificity, as shown in Table 2. Figure 5b depicts the area

Table 2. Parameters for the *A. niger* Data Sets Employed in the PLS-DA Classification Model

parameters	values
sensitivity	87%
specificity	88.9%
AUC	0.67
accuracy	89%
precision	87.7%

under the receiver operating characteristic curve (AUROC), which has a value close to 1, indicating the excellent performance of the model for the discrimination of the SERS spectral data sets. The curve is plotted between the false-positive and true-positive rates. Therefore, this model was used for the discrimination between nonmutated and mutated *A. niger* fungi by an AUROC score of 0.67.

3. CONCLUSIONS

Surface-enhanced Raman spectroscopy (SERS) with PCA and PLS-DA was employed to compare the nonmutated *A. niger*
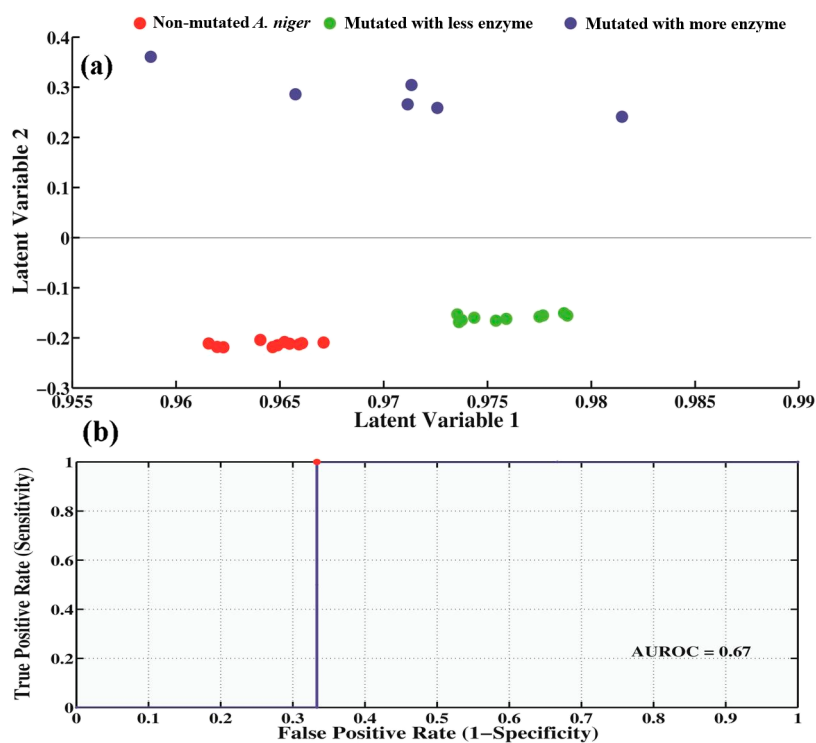
Figure 5. (a) PLS-DA score plot for SERS spectral data sets of unmutated *A. niger,* mutated *A. niger* with low enzyme production, and mutated *A. niger* with high enzyme production. (b) Area under the curve value for the PLS-DA model.

and the two types of mutated *A. niger* including the ones with low and high production of the cellulase enzyme. Different SERS spectral features associated with the biochemical changes taking place due to the mutation in the DNA of fungal mycelial cells are identified, including 622, 655, 738, 802, and 1331 cm^{-1}. This method could also discriminate the SERS data sets of nonmutated and mutated *A. niger*. A comparison of SERS data sets also provided unique features associated with the mutation. The PCA scores reported by the PC-1 value in the SERS spectral region of 500−1800 cm^{-1} accounted for nearly 99% of the variance, validating the categorization of three distinct data sets, each of which corresponds to a distinct class of the fungus *A. niger*. PLS-DA was employed for the successful discrimination with 89% accuracy, 87.7% precision, 88.9% specificity, 87% sensitivity, and an area under the receptive operating curve (AUROC) of 0.67.

4. MATERIALS AND METHODS

4.1. Sample Preparation. For the purpose of using CRISPR-Cas9-based genome editing, the endogenously isolated *A. niger* strain BNB01 was employed. Using the Internet web browser CHOPCHOP (http://chopchop.cbu.uib.no/), the 20 bp protospacer sequence-specific gRNA against the *creA* gene was developed.[31] In order to create the CRISPR-Cas9 gRNA expression vector, the plasmids pFC332 and pFC334 were employed by using USER cloning as previously described.[32]

For optimum growth, the parent and genetically modified *A. niger* strains were grown in Vogel's media with an initial pH of 5.0[33] for 48 h at 30 ± 1 °C in an orbital shaking incubator (at 120 rpm). Cell mass (mycelia) from the fungal growth culture was collected into 2 mL sterile microcentrifuge tubes, and the supernatant was separated by centrifugation at 6000 rpm (4430*g*) for 10 min at 4 °C.

4.2. Synthesis of Silver Nanoparticles (Ag NPs). The silver nanoparticles (Ag NPs) were prepared by a chemical reduction method. In this method, silver nitrate (AgNO$_3$) was used as the precursor. Trisodium citrate (Na$_3$C$_6$H$_5$O$_7$) was used as a capping ligand and reducing agent. For this, 100 mL of distilled water was taken in a beaker and 0.025 g of AgNO$_3$ was added to it. Then, this solution was heated on a hot plate at 90 °C temperature with continuous stirring until it started to boil. Then, 0.017 g of trisodium citrate was added to the boiling solution of silver nitrate. Boiling on the hot plate was continued until the volume of the solution was reduced up to 20 mL. Then, the beaker was removed from the hot plate and the solution of Ag NPs was transferred to another beaker and kept in the dark to cool down to room temperature. Centrifugation was performed at 6000 rpm for 10 min for the removal of the supernatant. Now, the synthesized Ag NPs were characterized through SEM and TEM,[21,34] and the results are provided in the Supporting Information.

4.3. SERS Acquisition. For SERS spectral acquisition of *A. niger* samples, a Raman spectrometer (Peak Seeker pro-785 Agiltron) was used. For this, 15 μL of the sample and 15 μL of Ag NPs were taken in an Eppendorf tube and incubated for 30 min. Then, the sample was placed on an aluminum slide. A 785 nm diode laser with a laser power of 50 mW was used, along with a 40× objective and an acquisition time of 15 s. As a result, 15 Raman spectra were collected from each sample.

4.4. SERS Data Preprocessing. MATLAB 7.8.0. R2009a[21] was used for the preprocessing of SERS spectral data of all of the isolated DNA samples from *A. niger* fungus. The SERS spectra were confined to the wavelength range of 400−1800 cm^{-1}. SERS data were taken in a matrix and preprocessed. The steps involved in the preprocessing include substrate removal, baseline correction, smoothing, and vector normalization. The Savitzky−Golay method[35] (order 7, 13

point window) was used for smoothening the spectra, and the substrate background was removed by the subtraction method. The baseline was corrected by a rubber band correction method.[36]

4.5. SERS Data Analysis. SERS spectral data sets were analyzed by means of principal component analysis (PCA) and partial least-squares discriminant analysis (PLS-DA). PCA is a model that can be created without any prior knowledge of the classes. It is a strategy for converting correlated variables into uncorrelated variables in a qualitative approach. This approach reduces the dimensionality of spectral data sets, while their variability remains the same. PC-1 is used to explain the dominant source of variability and PC-2 to explain the succeeding source of variability. The SERS spectra are interpreted using spectral feature assignments from the literature and mentioned in the peak assignment in Table 1. Principal component analysis was employed to elucidate the biochemical changes occurring in the nonmutated *A. niger* samples as compared with mutated samples. The PCA loadings can be considered as the orthogonal dimensions of biochemical differences that make it easier to distinguish various groups of SERS spectral data along their variability.

■ AUTHOR INFORMATION

Corresponding Authors

Muhammad Rizwan Javed − *Biocatalysis and Protein Engineering Research Group (BPERG), Department of Bioinformatics and Biotechnology, Government College University Faisalabad (GCUF), Faisalabad 38000, Pakistan*; Email: rizwan@gcuf.edu.pk

Haq Nawaz − *Department of Chemistry, University of Agriculture Faisalabad, Faisalabad 38000, Pakistan;* orcid.org/0000-0003-2739-4735; Email: haqchemist@yahoo.com

Muhammad Irfan Majeed − *Department of Chemistry, University of Agriculture Faisalabad, Faisalabad 38000, Pakistan;* orcid.org/0000-0003-0506-6060; Email: irfan.majeed@uaf.edu.pk

Authors

Muhammad Wasim − *Department of Chemistry, University of Agriculture Faisalabad, Faisalabad 38000, Pakistan*

Usman Ghaffar − *Department of Chemistry, University of Agriculture Faisalabad, Faisalabad 38000, Pakistan*

Anam Ijaz − *Biocatalysis and Protein Engineering Research Group (BPERG), Department of Bioinformatics and Biotechnology, Government College University Faisalabad (GCUF), Faisalabad 38000, Pakistan*

Shazra Ishtiaq − *Department of Chemistry, University of Agriculture Faisalabad, Faisalabad 38000, Pakistan*

Nimra Rehman − *Department of Chemistry, University of Agriculture Faisalabad, Faisalabad 38000, Pakistan*

Rabeea Razaq − *Department of Chemistry, University of Agriculture Faisalabad, Faisalabad 38000, Pakistan*

Sobia Younas − *Department of Chemistry, University of Agriculture Faisalabad, Faisalabad 38000, Pakistan*

Aqsa Bano − *Department of Chemistry, University of Agriculture Faisalabad, Faisalabad 38000, Pakistan*

Naeema Kanwal − *Department of Chemistry, University of Agriculture Faisalabad, Faisalabad 38000, Pakistan*

Muhammad Imran − *Department of Chemistry, Faculty of Science, King Khalid University, Abha 61413, Saudi Arabia;* orcid.org/0000-0003-4072-4997

Complete contact information is available at:
https://pubs.acs.org/10.1021/acsomega.3c09563

Author Contributions

‖M.W. and U.G. contributed equally to this work.

Notes

The authors declare no competing financial interest.

■ ACKNOWLEDGMENTS

■ REFERENCES

(1) Pritesh, P.; Bhaumik, D.; Ankit, S.; Ketankumar, P.; Subramanian, R. Modified and simple method for isolation of genomic DNA from fungal culture. *Afr. J. Microbiol. Res.* **2014**, *8* (22), 2261−2263.

(2) Perfect, J.; Cox, G.; Lee, J.; Kauffman, C.; De Repentigny, L.; Chapman, S.; Morrison, V. A.; Pappas, P.; Hiemenz, J.; Stevens, D. The impact of culture isolation of Aspergillus species: a hospital-based survey of aspergillosis. *Clin. Infect. Dis.* **2001**, *33* (11), 1824−1833.

(3) Baker, S. E. *Aspergillus niger* genomics: past, present and into the future. *Med. Mycol.* **2006**, *44*, S17−S21.

(4) Saif, F.; Yaseen, S.; Alameen, A.; Mane, S.; Undre, P. Identification and characterization of Aspergillus species of fruit rot fungi using microscopy, FT-IR, Raman and UV−Vis spectroscopy. *Spectrochim. Acta, Part A* **2021**, *246*, No. 119010.

(5) ur Rahman, M.; et al. Antimycotic activity of essential oil of Rosmarinus officinalis on asexual reproductive stages of foodstuff fungi. *Int. J. Pure Appl. Biosci.* **2017**, *5* (5), 1−9.

(6) Singhania, R. R.; Sukumaran, R. K.; Patel, A. K.; Larroche, C.; Pandey, A. Advancement and comparative profiles in the production technologies using solid-state and submerged fermentation for microbial cellulases. *Enzyme Microb. Technol.* **2010**, *46* (7), 541−549.

(7) Saini, R.; Saini, J. K.; Adsul, M.; Patel, A. K.; Mathur, A.; Tuli, D.; Singhania, R. R. Enhanced cellulase production by Penicillium oxalicum for bio-ethanol application. *Bioresour. Technol.* **2015**, *188*, 240−246.

(8) Schuster, M.; Kahmann, R. CRISPR-Cas9 genome editing approaches in filamentous fungi and oomycetes. *Fungal Genet. Biol.* **2019**, *130*, 43−53.

(9) Ahmad, I.; Khan, M. S. A.Microscopy in Mycological Research with Especial Reference to Ultrastructures and Biofilm Studies. In *Current Microscopy Contributions to Advances in Science and Technology*; Formatex Research Center: Spain, 2012; pp 646−659.

(10) Naqvi, S. Z. H.; Kiran, U.; Ali, M. I.; Jamal, A.; Hameed, A.; Ahmed, S.; Ali, N. Combined efficacy of biologically synthesized silver nanoparticles and different antibiotics against multidrug-resistant bacteria. *Int. J. Nanomed.* **2013**, 3187−3195.

(11) Hua, Y.; Pan, R.; Bai, X.; Wei, B.; Chen, J.; Wang, H.; Zhang, H. Aromatic polyketides from a symbiotic strain Aspergillus fumigatus D and characterization of their biosynthetic gene D8. t287. *Mar. Drugs* **2020**, *18* (6), No. 324.

(12) Maquelin, K.; Kirschner, C.; Choo-Smith, L.-P.; Ngo-Thi, N.; Van Vreeswijk, T.; Stammler, M.; Endtz, H.; Bruining, H.; Naumann, D.; Puppels, G. Prospective study of the performance of vibrational spectroscopies for rapid identification of bacterial and fungal pathogens recovered from blood cultures. *J. Clin. Microbiol.* **2003**, *41* (1), 324−329.

(13) Efrima, S.; Zeiri, L. Understanding SERS of bacteria. *J. Raman Spectrosc.* **2009**, *40* (3), 277−288.

(14) Farazkhorasani, F. *Raman and SERS Studies of Filamentous Fungi*; Royal Society of Chemistry, 2012.

(15) Dina, N. E.; Gherman, A. M. R.; Chiş, V.; Sârbu, C.; Wieser, A.; Bauer, D.; Haisch, C. Characterization of clinically relevant fungi via

SERS fingerprinting assisted by novel chemometric models. *Anal. Chem.* **2018**, *90* (4), 2484−2492.

(16) Ciloglu, F. U.; Saridag, A. M.; Kilic, I. H.; Tokmakci, M.; Kahraman, M.; Aydin, O. Identification of methicillin-resistant Staphylococcus aureus bacteria using surface-enhanced Raman spectroscopy and machine learning techniques. *Analyst* **2020**, *145* (23), 7559−7570.

(17) Xia, J.; Li, W.; Sun, M.; Wang, H. Application of SERS in the Detection of Fungi, Bacteria and Viruses. *Nanomaterials* **2022**, *12* (20), No. 3572.

(18) Gherman, A. M. R.; Dina, N. E.; Chiş, V.; Wieser, A.; Haisch, C. Yeast cell wall−Silver nanoparticles interaction: A synergistic approach between surface-enhanced Raman scattering and computational spectroscopy tools. *Spectrochim. Acta, Part A* **2019**, *222*, No. 117223.

(19) Tariq, A.; Javed, M. R.; Majeed, M. I.; Nawaz, H.; Rashid, N.; Yousaf, S.; Ijaz, A.; ul Huda, N.; Tahseen, H.; Naman, A.; et al. Characterization of *Aspergillus niger* DNA by Surface-Enhanced Raman Spectroscopy (SERS) with Principal Component Analysis (PCA) and Partial Least Square Discriminant Analysis (PLS-DA) with Application for the Production of Cellulase. *Anal. Lett.* **2023**, *57*, 1123−1136.

(20) De Gussem, K.; Vandenabeele, P.; Verbeken, A.; Moens, L. Raman spectroscopic study of Lactarius spores (Russulales, Fungi). *Spectrochim. Acta, Part A* **2005**, *61* (13−14), 2896−2908.

(21) ul Huda, N.; Wasim, M.; Nawaz, H.; Majeed, M. I.; Javed, M. R.; Rashid, N.; Iqbal, M. A.; Tariq, A.; Hassan, A.; Akram, M. W.; et al. Synthesis, Characterization, and Evaluation of Antifungal Activity of 1-Butyl-3-hexyl-1 H-imidazol-2 (3 H)-selenone by Surface-Enhanced Raman Spectroscopy. *ACS Omega* **2023**, *8* (39), 36460−36470.

(22) Kashif, M.; Majeed, M. I.; Hanif, M. A.; ur Rehman, A. Surface Enhanced Raman Spectroscopy of the serum samples for the diagnosis of Hepatitis C and prediction of the viral loads. *Spectrochim. Acta, Part A* **2020**, *242*, No. 118729.

(23) Saleem, M.; Majeed, M. I.; Nawaz, H.; Iqbal, M. A.; Hassan, A.; Rashid, N.; Tahir, M.; Raza, A.; ul Hassan, H. M.; Sabir, A.; et al. Surface-enhanced Raman spectroscopy for the characterization of the antibacterial properties of imidazole derivatives against bacillus subtilis with principal component analysis and partial least squares−discriminant analysis. *Anal. Lett.* **2022**, *55* (13), 2132−2146.

(24) Perez, J. C. R.; Dos Reis, T. A.; de Almeida Rizzutto, M. Identifying and detecting Entomopathogenic fungi using Surface-enhanced Raman spectroscopy. *Braz. J. Anim. Environ. Res.* **2021**, *4* (4), 4833−4851.

(25) Long, Y.; Huang, W.; Wang, Q.; Yang, G. Green synthesis of garlic oil nanoemulsion using ultrasonication technique and its mechanism of antifungal action against Penicillium italicum. *Ultrason. Sonochem.* **2020**, *64*, No. 104970.

(26) Guo, Z.; Wang, M.; Barimah, A. O.; Chen, Q.; Li, H.; Shi, J.; El-Seedi, H. R.; Zou, X. Label-free surface enhanced Raman scattering spectroscopy for discrimination and detection of dominant apple spoilage fungus. *Int. J. Food Microbiol.* **2021**, *338*, No. 108990.

(27) Raza, A.; Parveen, S.; Majeed, M. I.; Nawaz, H.; Javed, M. R.; Iqbal, M. A.; Rashid, N.; Haider, M. Z.; Ali, M. Z.; Sabir, A.; et al. Surface-enhanced Raman spectral characterization of antifungal activity of selenium and zinc based organometallic compounds. *Spectrochim. Acta, Part A* **2023**, *285*, No. 121903.

(28) Nawaz, H.; Rashid, N.; Saleem, M.; Asif Hanif, M.; Irfan Majeed, M.; Amin, I.; Iqbal, M.; Rahman, M.; Ibrahim, O.; Baig, S.; et al. Prediction of viral loads for diagnosis of Hepatitis C infection in human plasma samples using Raman spectroscopy coupled with partial least squares regression analysis. *J. Raman Spectrosc.* **2017**, *48* (5), 697−704.

(29) Witkowska, E.; Jagielski, T.; Kamińska, A.; Kowalska, A.; Hryncewicz-Gwóźdź, A.; Waluk, J. Detection and identification of human fungal pathogens using surface-enhanced Raman spectroscopy and principal component analysis. *Anal. Methods* **2016**, *8* (48), 8427−8434.

(30) Akram, M.; Majeed, M. I.; Nawaz, H.; Rashid, N.; Javed, M. R.; Ali, M. Z.; Raza, A.; Shakeel, M.; ul Hasan, H. M.; Ali, Z.; et al. Surface-enhanced Raman spectroscopy for characterization of filtrate portions of blood serum samples of typhoid patients. *Photodiagn. Photodyn. Ther.* **2022**, *40*, No. 103199.

(31) Labun, K.; Montague, T. G.; Gagnon, J. A.; Thyme, S. B.; Valen, E. CHOPCHOP v2: a web tool for the next generation of CRISPR genome engineering. *Nucleic Acids Res.* **2016**, *44* (W1), W272−W276.

(32) Nødvig, C. S.; Nielsen, J. B.; Kogle, M. E.; Mortensen, U. H. A CRISPR-Cas9 system for genetic engineering of filamentous fungi. *PLoS One* **2015**, *10* (7), No. e0133085.

(33) Javed, M. R.; Rashid, M. H.; Riaz, M.; Nadeem, H.; Qasim, M.; Ashiq, N. Physiochemical and thermodynamic characterization of highly active mutated Aspergillus niger *β*-glucosidase for lignocellulose hydrolysis. *Protein Pept. Lett.* **2018**, *25* (2), 208−219.

(34) Ramirez-Perez, J. C.; Reis, T. A.; Olivera, C. L.; Rizzutto, M. A. Impact of silver nanoparticles size on SERS for detection and identification of filamentous fungi. *Spectrochim. Acta, Part A* **2022**, *272*, No. 120980.

(35) Butler, H. J.; Smith, B. R.; Fritzsch, R.; Radhakrishnan, P.; Palmer, D. S.; Baker, M. J. Optimised spectral pre-processing for discrimination of biofluids via ATR-FTIR spectroscopy. *Analyst* **2018**, *143* (24), 6121−6134.

(36) Saleem, M.; Majeed, M. I.; Nawaz, H.; Iqbal, M. A.; Hassan, A.; Rashid, N.; Tahir, M.; Raza, A.; ul Hassan, H. M.; Sabir, A.; et al. Surface-Enhanced Raman Spectroscopy for the Characterization of the Antibacterial Properties of Imidazole Derivatives against Bacillus subtilis with Principal Component Analysis and Partial Least Squares−Discriminant Analysis. *Anal. Lett.* **2022**, *55*, 2132−2146.